

Mini review

Electrochemical Biosensors with Silver Nanoparticles as Signal Labels

Cai-Xia Yu^{1,*}, Fan Xiong¹ and Lei-Lei Liu^{2,*}

¹ Henan Province of Key Laboratory of New Optoelectronic Functional Materials, College of Chemistry and Chemical Engineering, Anyang Normal University, Anyang, Henan 455000, People's Republic of China

² School of Environment and Material Engineering, Yantai University, Yantai 264005, People's Republic of China

*E-mail: yucaixiachem@163.com (C. X. Yu), liuleileimail@163.com (L. L. Liu)

Received: 6 January 2020 / Accepted: 12 February 2020 / Published: 10 April 2020

The fabrication of electrochemical biosensors with high sensitivity and selectivity has attracted increasing attention during the past decades. Due to their excellent chemical and electrical properties, especially low-redox potential and highly characteristic solid-state Ag/AgCl process, silver nanoparticles (AgNPs) have been extensively employed to design novel and efficient electrochemical sensing methods. Herein, we summarize the applications of AgNPs as electroactive labels in biosensors. This review aims to provide a snapshot of recent development of AgNPs-based electrochemical sensors and to illustrate their benefits for biological and biomedical applications.

Keywords: silver nanoparticles; signal amplification; electrochemical biosensors; silver deposition; biometallization

1. INTRODUCTION

Over the past decades, there is growing demand to identify less abundant biomolecules related to disease diagnosis, clinical treatment, food safety, and homeland security. Consequently, a wide variety of biosensors based on different analytical techniques have been developed, including fluorescence, electrochemistry, surface-enhanced Raman scattering, and colorimetry [1]. Among those conventional detection techniques, electrochemical bioanalysis has aroused great interests because of their analytical characteristics including simplicity, high sensitivity, low cost and real-time detection. To meet the growing demands for ultrasensitive detection, researchers have designed a number of electrochemical strategies for the development of nanomaterials-based electrochemical sensors.

As well known, per nanoparticle label (semiconductor quantum dots (QDs) and metal nanoparticles (NPs)) consists of thousands of atoms, which can be electrochemically oxidized or reduced. Thus, they can provide considerable signal amplification of the transduction signal of a recognition event, causing a dramatic increase in electrochemical biosensors. Therefore, the quantification of target molecules can be indirectly achieved by the electrochemical detection of nanoparticles labels. Normally, due to their intrinsic stability, the captured QDs and metal NPs should be dissolved by strong acids or oxidants to produce a “burst” of metal ions, which can further be detected via voltammetry [2-4]. However, the dissolution step and metal preconcentration before electrochemical detection are complicated and time-consuming. To simplify the detection steps and reduce the detection time, researchers have putted numerous attentions into designing and exploiting new nanoprobe. For example, Zhu’s group reported series of electrochemical bioassays by using metal-functionalized titanium phosphate nanospheres (TiP-metal ion) as labels to avoid acid dissolution and preconcentration [5-8]. Moreover, other electroactive metal ions (such as cadmium, lead, silver, zinc and copper)-loading NPs are also widely employed as signal reporters for the development of electrochemical biosensors, including metal-organic framework [9-12], graphene oxide (GO) [13], poly(amidoamine) dendrimer [14] and alginate nanobeads [15].

On the other hand, metal nanoparticles can also be utilized as nano-tracers. Gold nanoparticles (AuNPs) are the most widely used for signal amplification because of ease to synthesis and functionalization, and high stability. Wang’s group described a AuNPs-based electrochemical sensor for DNA hybridization, based on electrochemical stripping detection of AuNPs [16]. In this study, following the hybridization of a biotinylated target and oligonucleotide probe-coated magnetic beads (MB), the streptavidin-coated AuNPs was captured and dissolved. The dissolved gold ions were detected by potentiometric stripping method. However, the potential region of the electrooxidation of AuNPs is close to the potential limit in aqueous electrolyte media and thus the background process is dominant. Therefore, the captured AuNPs labels were oxidized chemically using HBr/Br₂ or electrochemically in HCl [17, 18].

As another most utilized noble metal NPs, silver nanoparticles (AgNPs) possesses significant electrochemical reactivity, and exhibits sharp oxidation peaks and low-redox potentials in aqueous solution, which make them more excellent than AuNPs in electrochemical biosensors [19]. Fang and co-workers reported an electrochemical DNA hybridization detection assay based on AgNPs as the labels, in which only concentrated HNO₃ was needed to dissolve AgNPs, rather than more severe conditions (1 M HBr containing 0.1 mM Br₂) [20]. Moreover, Wang’s group demonstrated that metallic silver label could be directly electrochemically oxidized into silver ions in solid-state or in aqueous solution through differential pulse voltammetry (DPV) [21, 22]. More interestingly, in 2009, Ying and co-workers confirmed that the highly characteristic solid-state Ag/AgCl process associated with AgNPs in an aqueous KCl electrolyte medium could be introduced into electrochemical biosensors with the minimal background [23, 24]. Compared with the Ag(solid) → Ag⁺(solution) + e⁻ stripping process, the process of Ag(solid) + Cl⁻(solution) → AgCl(solid) + e⁻ solid-state occurs in a viable potential region separated from the oxygen reduction potential. Singh et al. further confirmed that this process took place via a redox-driven solid-state phase transformation and AgNPs was reversible oxidized into silver halide NPs [25].

In this review, we focus on the recent development of signal amplification strategies based on using AgNPs as the electroactive tag without the need of oxidants, mainly on the solid-state phase transformation of AgNPs in aqueous halide solutions or in hydroxide solutions. The strategies using AgNPs as the electroactive tags in electrochemical biosensors encompass six main types: (1) individual AgNP, (2) AgNPs aggregates, (3) AgNPs-based nanocomposites, (4) nanomaterial-promoted reduction of silver ions, (5) DNA-based biometallization, and (6) ALP-catalyzed silver deposition.

2. STRATEGIES OF SILVER-BASED LABELS

2.1 Individual AgNP

An electrochemical DNA sensor, based on neutral peptide nucleic acid (PNA) as probes and amine-functionalized positively charged AgNPs as electroactive labels, was reported by Zhang et al. through the highly characteristic solid-state Ag/AgCl reaction [23]. Neutral PNA probes were chosen as capture probes to comparatively reduce background signal. After hybridization between PNA and target DNA, a negatively charged surface was generated, thus allowing for the adsorption of positively charged AgNPs through electrostatic interaction. Due to the sharper and more intensive peak of solid-state voltammogram, even when 10 fM of DNA was added, the signal was still well distinguished. Doxorubicin-labelled AgNPs were also utilized by them to intercalate into hybridized ds-DNA for the electrochemical detection of short DNA oligonucleotide of avian flu virus H5N1 [26]. After that, many novel and elaborate works based on the highly characteristic solid-state Ag/AgCl reaction were worldily reported, especially combining with various powerful nuclease-assisted target recycling and DNA amplification techniques. Zhuang and co-workers employed DNA-based hybridization chain reaction (HCR) to form long-range ds-DNA nanostructures and absorb more positively charged AgNPs for signal amplification [27]. Gao and co-workers proposed a novel dual-amplification strategy based on exonuclease III-assisted target recycling and rolling circle amplification (RCA) [28]. The long, amplified ss-DNA products could hybridize with the detection probe-modified AgNPs, thereby binding the multiplication of AgNPs on the electrode surface for subsequent electrochemical strip analysis. Miao and co-workers reported a target induced recycling amplification strategy for the identification of cellular microRNA by integrating strand displacement polymerization and nicking-endonuclease-mediated cleavage [29]. In the absence of microRNA, blocker DNA partially hybridized with AgNPs-labelled signal DNA with a restriction site of Nt.BbvCI, and the hybrid was cleaved by the enzyme, resulting in leaving of AgNPs and decrease of electrochemical signals. However, in the presence of microRNA, it would hybridize with blocker DNA from the hybrid on the electrode surface with higher priority. Then, after the extension reaction by the Klenow fragment, microRNA was displaced and further hybridized with more blocker DNA circularly. Therefore, numerous single-stranded signal DNA probes existed on the electrode surface and immobilized AgNPs would produce intense silver stripping current. They also fabricated an electrochemical approach for microRNA analysis, by combining DNA/microRNA/DNA hybridization and ligation/denaturation procedures

[30]. After the denaturation, only the ligated product of the adjacent DNA1 and NH₂-functionalized DNA2 was remained on the electrode surface and captures AgNPs via silver-amino chemistry.

According to the previous reports, tetrahedral DNA nanostructures largely enhance the accessibility and molecular recognition efficiency [31, 32]. After modification with sulfur at three vertices, they can be rapidly and firmly adsorbed at gold surfaces, avoiding the introduction of spacer molecules and simplifying the immobilization steps. Miao and coworkers proposed series of interesting strategies for the detection of molecules of interest, based on tetrahedral DNA nanostructure [33, 34]. For example, with the aid of microRNA, AuNPs modified with capture DNA first were bound on the electrode surface and initiated hybridization chain reaction by employing AgNP-labeled HCR-H1 and H2 as fuel strands. As shown in Figure 1A, strand displacement polymerization and catalytic recycling of microRNA were also combined to detect microRNA [35]. In the presence of microRNA, the stem of tetrahedron A was released and hybridized with the AgNP-labeled signal probe. Then, Klenow fragment initiated the polymerization and lengthening of signal probe, releasing microRNA to induce more loops opening and more signal probe hybridizing. Multiplication of AgNP-labeled signal probes was recruited on the electrode surface and intensive electrochemical signals were generated. The developed biosensor showed high sensitivity with the LOD down to 0.4 fM. Based on the catalysis of exonuclease I (Exo I) and nicking endonuclease (NEase), they also designed an electrochemical biosensor for coralyne detection [36]. In this study, the 5'-terminus of the pendant DNA sequence on the top of the tetrahedron is conjugated with AgNPs as electrochemical species. The pendant sequence could hybridize with the complex of DNA probe 1 and coralyne, and then be cleaved into two pieces by NEase. Thus, the complex was released and subsequently more pendant sequence was nicked. Finally, the number of AgNPs releasing from the electrode surface would be greatly increased and the declined electrochemical signal is thus amplified. Recently, aiming to detect extremely low abundant DNAs, a smart bipedal DNA walking machine was designed on the surface of the DNA tetrahedron-modified electrode surface (Figure 1B) [37]. First, in the presence of target DNA, magnetic separation and strand displacement amplification were conducted to produce plenty of probe B. Under the help of probe B and in the presence of probes C and D, and Pb²⁺, the walking process is proceeded on the electrode surface and many amino groups of the DNA track were eliminated, making AgNPs unable to be absorbed. Therefore, the LOD of 0.22 fM is achieved with triple signal amplification.

Electrochemical immunosensors based on AgNPs with the molecular recognizing property have attracted considerable interest in recent years because of their high sensitivity, low-cost and inherent miniaturization [38]. For example, Hao et al. reported an electrochemically direct stripping approach for human IgG detection based on the goat-anti-human IgG labeled AgNPs by DPV method [39]. Besides, Yin et al. fabricated chitosan (CS)-protected AgNPs (AgNPs-CS) to modify the electrode for the subsequently decoration of AuNPs and antibody on its surface to develop an immunosensor for human IgG [40]. AuNPs could greatly enhance the silver stripping current and provide sites for the antibody immobilization. After the sandwich immunoreaction, the formed dielectric antibody-antigen immunocomplex decreased the stripping current of AgNPs. Moreover, due to its low semiconducting conductivity, the captured silica nanoparticles on the electrode surface further increased the electrochemical impedance and amplified the inhibition of the stripping signal of

AgNPs, thus leading to the great enhancement of the sensitivity. The immunosensor showed a good linear range from 1.0 pg/mL to 100 ng/mL with a low LOD of 0.67 pg/mL.

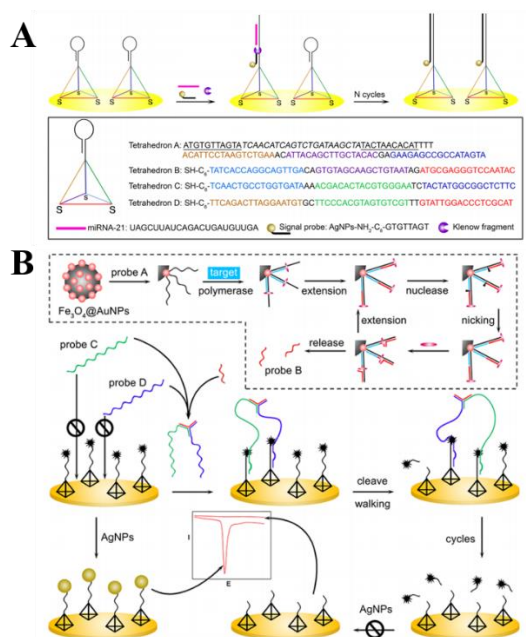


Figure 1. (A) Schematic illustration of the tetrahedral DNA nanostructure-based microRNA biosensor. Reprinted with permission from [35]. Copyright 2015 American Chemical Society. (B) Illustration of the bipedal DNA walker based electrochemical genosensor. Reprinted with permission from [37]. Copyright 2019 American Chemical Society.

As we all known, sensitive cell analysis is of importance for early diagnosis of diseases. Yazdanparast et al. presented a sensitive and selective method for detection of human breast cancer cells and MUC1 biomarker based on dual-aptamer to link aptamer-labelled AgNPs to the electrode surface [41]. Similarly, Meng et al. employed Cys-Arg-Gly-Asp-Ser (CRGDS) modified AgNPs to detect cancer cells on a DNA tetrahedron nanostructure assembled gold electrode [42]. Different from the currently used versatile probes using lectin, Zhang et al. synthesized *p*-sulfonatocalix[4]-arene-modified silver nanoparticles (*p*SC4-AgNPs) and explored it as a universal nanoprobe for cell analysis, in which *p*SC4 can recognize and bind to various amino acid residues on the cell membrane protein (Figure 2A) [43]. When HepG2 is captured on the electrode with the aid of aptamer, *p*SC4-AgNPs coordinate with the immobilized cell and give a sensitive electrochemical signal. The established method exhibited a wider detection range from 5 to 2.5×10^5 cells with a LOD of 5 cells, lower than other reported methods for electrochemical analysis of cells. By using self-assembling peptide-based multifunctional nanofibers (MNFs), Tang et al. proposed an electrochemical method to identify breast cancer stem cells (BCSCs) (Figure 2B) [44]. The peptide probe consists of three parts: N₃ group at the N-terminal for recruiting AgNPs, KLVFF peptide motif for controllable formation of β -sheet structured nanofibers, and the CD44 binding peptide (CD44BP) motif for stemness recognition. After the AS1411 aptamer immobilized on the electrode surface captured BCSCs, MNFs

selectively recognized BCSCs through the binding with CD44. Next, a large number of azide groups on MNFs would be ligated with dibenzocyclooctyne-functionalized AgNPs as labels. This method could detect target cells as low as 6 cells/mL and have a wide linear range from 10 to 5×10^5 cells/mL.

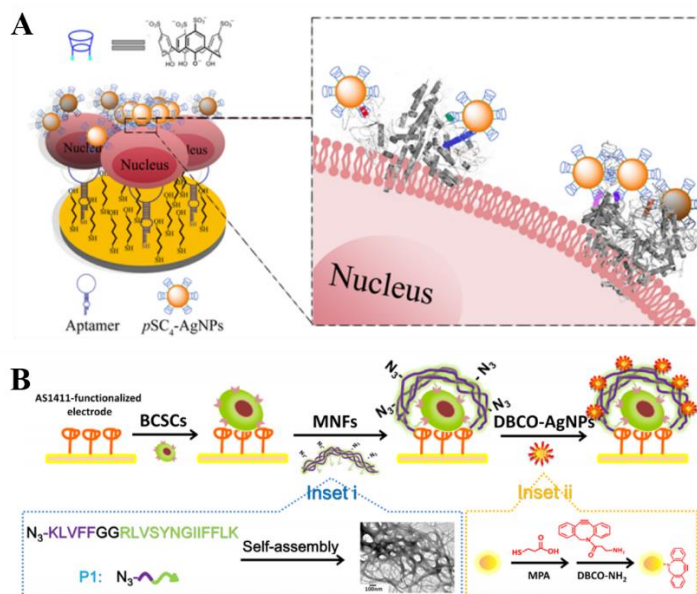


Figure 2. (A) Schematic illustration for mechanism of cell electrochemical detection by using pSC_4 -AgNPs as a universal and sensitive electrochemical probe. Reprinted with permission from [43]. Copyright 2019 American Chemical Society. (B) Schematic illustration of the multifunctional nanofiber-assisted electrochemical identification of BCSCs. Reprinted with permission from [44]. Copyright 2019 American Chemical Society.

Small molecules can also be used as the bridge to immobilize AgNPs on the electrode surface through hydrogen bond, metal-S bond and specific chemical reaction. Miao et. al employed melamine-functionalized AgNPs (M-AgNPs) as the electroactive probe for electrochemical sensing of clenbuterol (Figure 3) [45]. Clenbuterol could interact with melamine modified gold electrode and further capture M-AgNPs on the surface of the electrode via the hydrogen-bonding interactions between clenbuterol and melamine, forming a sandwich structure. This method achieved a wide detection range from 10 pM to 100 nM and a low detection limit of 10 pM. Cui et al. reported an electrochemical sensor for the detection of Cu^{2+} by the assembly of AgNPs at dithiobis[succinimidylpropionate] modified Au nanoparticles (DSP-AuNPs), regulated by copper-catalyzed oxidation of cysteamine (Cys) [46]. Cys could link citrate-stabilized AgNPs and DSP-AuNPs on the electrode surface via Ag-S bond and the reaction between DSP and Cys. In the presence of Cu^{2+} , Cys was oxidized by dissolved oxygen to form cystamine, inhibiting the loading of AgNPs on the DSP terminated sensor and decreasing the electrochemical stripping signal of AgNPs.

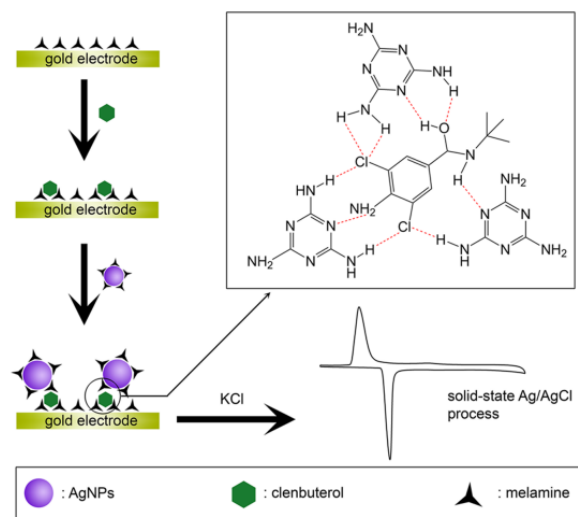


Figure 3. Schematic representation of the melamine functionalized silver nanoparticles-based electrochemical biosensor. Reprinted with permission from [45]. Copyright 2014 American Chemical Society.

2.3 AgNPs aggregates

Normally, aggregation of individual metal NPs can change the LSPR wavelength of NPs and accompany with the change of the color of the solution (such as from red wine to blue or purple), which is the basic mechanism of colorimetric sensors. Interestingly, Wei et al. converting this liquid-phase colorimetric assay into enhanced surface-tethered electrochemical analysis, with greatly amplified electrochemical signal [47]. Because, one target can capture one AgNP, and bridge molecules or crosslinkers was introduced to transform large numbers of AgNPs into network architecture, thus leading to greatly amplified electrochemical signal based on the solid-state Ag/AgCl reaction from AgNP aggregates to AgCl.

Li et al. fabricated AgNPs aggregates as tags through hybridization-induced assembly of DNA-AgNPs for ultrasensitive electrochemical detection of multiplexed DNA target (Figure 4A) [48]. Through sandwich hybridization format, the AgNPs aggregate tag was specifically recruited to a gold electrode surface via target DNA. Compared to a single nanoparticle label, this novel tag exhibited excellent electroactive property and produced 10^3 -fold signal amplification in the DPV method. However, AgNPs aggregate tags were synthesized through hybridization before the sandwich assay, which may affect the uniformity of the size of the silver aggregate. Therefore, they also combining the *in situ* hybridization-inducing aggregate of DNA-AgNPs with differential pulse stripping voltammetry (DPSV) method for detection of platelet-derived growth factor (PDGF-BB) (Figure 4B) [49]. AgNPs were modified with hybridization DNA and aptamers. After PDGF-BB was captured by the aptamer-modified electrode, two kinds of DNA-AgNPs were simultaneously introduced for specifically recognizing PDGF-BB and forming the AgNPs aggregate via *in situ* hybridization of DNA. This *in situ* hybridization-inducing aggregate as tracing tags were further applied to develop multiplied proteins assays for PDGF-BB and thrombin. Besides the unique recognition and hybridization property of DNA, the specific interaction between biotin and streptavidin (SA) can be utilized to induce metal

NPs aggregate, which have been widely used to develop bioassays for various molecules of interest. Jiang et al. reported an electrochemical detection of *Bacillus thuringiensis* transgenic sequence by using SA as bridge molecule to *in situ* induce biotin-AgNPs aggregates [50].

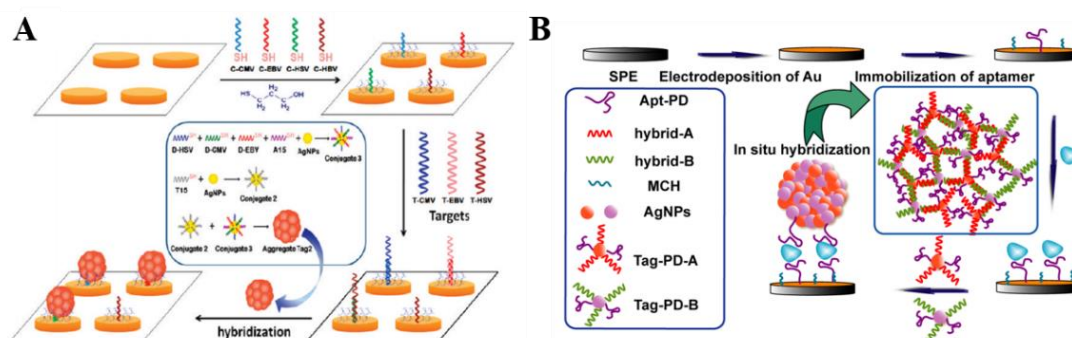


Figure 4. (A) Schematic illustration of the electrochemical multiplexed assay with silver nanoparticle conjugates and preparation of the aggregates. Reprinted with permission from [48]. Copyright 2010 American Chemical Society. (B) Schematic illustration of the strategy for the electrochemical assay of protein with signal amplification through AgNPs aggregate induced by in situ hybridization on SPE Array. Reprinted with permission from [49]. Copyright 2014 American Chemical Society.

Wei et al. synthesized thymine-functionalized AgNPs (Ag-T) nanoprobe as the electrochemical sensing unit for Hg^{2+} detection (Figure 5A) [47]. Hg^{2+} ions could couple Ag-T nanoprobe on a thymine-monolayer-modified gold electrode through T- Hg^{2+} -T coordination. Surface-tethered Ag-T nanoprobe can capture more ions and other Ag-T nanoprobe, leading to the formation of an Ag-T- Hg^{2+} -T-Ag architecture on the electrode surface. Under optimized conditions, Hg^{2+} ions were quantitatively detected by monitoring the LSV responses of Ag NPs in the network architecture. This simple but novel principle of analyte-induced aggregation of NPs can be used as a signal amplification strategy for the design of other sensors with significantly improved detection sensitivity. For example, Zhou et al. reported a 4-mercaptopbenzoic acid (MBA)-modified AgNPs-enhanced electrochemical sensor for the detection of Cu^{2+} , in which Cu^{2+} could chelated with the -COOH of MBA and trigger the formation of AgNPs-MBA- Cu^{2+} -MBA-AgNPs architecture on the electrode surface [51]. Similarly, low trace As(III) was dual-modally (electrochemical and colorimetric) detected by using multi-ligands functionalized AgNPs [52]. Besides as the analyte, metal ions could be used as a mediator to trigger the formation of aggregates during those type assays. Zhao et al. used electroactive Au@AgNPs as electrochemical tags and Cu^{2+} ions as mediators to the sensitive and accurate quantification of D-/L-Trp (Figure 5B) [53]. The binding constant of NPs and D-Trp was higher than that of NPs and L-Trp. The adsorbed affinity of D-Trp and Cu^{2+} was stronger than that of L-Trp and Cu^{2+} . Thus, the increasing amounts of D-Trp would cause more Au@AgNPs assembling to dimers, trimers, and even network architecture on the electrode with the aid of Cu^{2+} , generating amplified DPV signals. This established electrochemical chiral sensor achieved a LOD of 1.21 pM for D-Trp.

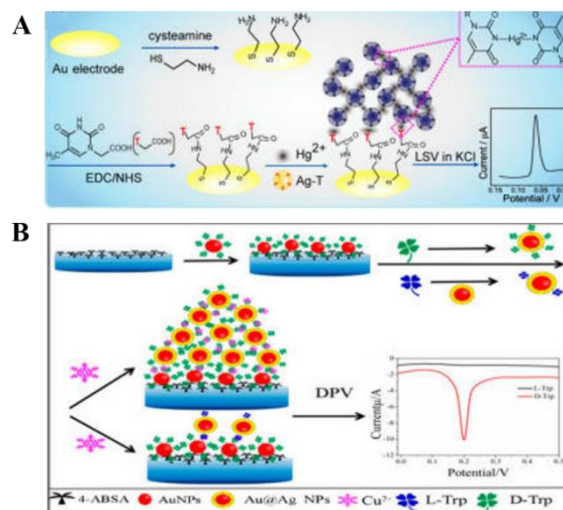


Figure 5. (A) Illustration of an electrochemical Hg^{2+} sensor based on analyte-induced aggregation of Ag-T nanoprobes. Reprinted with permission from [47]. Copyright 2015 American Chemical Society. (B) Illustration of electroactive Au@AgNP assembly driven signal amplification for ultrasensitive chiral discrimination of D-/L-Trp. Reprinted with permission from [53]. Copyright 2019 American Chemical Society.

Generally, small organic molecules, which can induce the aggregation of NPs, can also be employed to develop novel electrochemical sensors/biosensors, based on analyte-induced aggregation of NPs. Boronic acids can bind with α -hydroxycarboxylate acids and o-diphenol/diol-containing molecules, to form five or six-membered cyclic boronate ester. Therefore, boronic acids containing in molecules or nanomaterials have been widely used as the recognition group for sensing of biomolecules, such as catechol derivatives, sugars, RNA, nucleosides and glycoproteins [54, 55]. Moreover, other specific functional groups (such as thiol, amine and boronic acid) can be added into boronic acid-containing molecules, which can be used as a cross-linker between different molecules or NPs. We and Liu's groups have done some interesting works based on the boronic acids-induced NPs aggregation [56-60]. For example, we reported a label-free and highly sensitive method for the detection of miRNAs based on the formation of boronate ester covalent bonds (Figure 6A) [59]. After the hybridization between miRNAs and the thiolated hairpin-like DNA probe on the gold electrode, 4-mercaptophenylboronic acid (MPBA) was attached onto the 3'-terminal of miRNAs through the formation of a boronate ester bond and then captured AgNP via the Ag-S interaction. Then, free MPBA molecules in solution induced the *in situ* assembly of AgNPs on electrode surface through the covalent interactions between α -hydroxycarboxylate of citrate and boronate of MPBA and the formation of Ag-S bonds. The detection limit of this method was found to be 20 aM. Besides, Xia et. al reported an amperometric method for the analysis of glycoprotein based on the AgNPs-MPBA-AgNPs network architecture (Figure 6B) [58]. After being captured by the DNA aptamer-modified gold electrode, glycoprotein reacted with MPBA through the formation of boronate esters, then resulting in the formation of a network of AgNPs as redox reporters. With this strategy, Liu and co-workers designed different electrochemical strategies for the detection of protein kinase activity and protease

[60]. For instance, in one design, after the bound peptides were phosphorylated by tyrosine kinase Src with using adenosine 5-[γ -thio] triphosphate (ATP-S) as the co-substrate, the thiophosphate peptides could specifically conjugate the network of AgNPs to the electrode *via* the Ag-S interaction [61]. In another strategy, after tyrosine residues of peptides on electrode surface were oxidized by tyrosinase to form o-diphenol moieties, MPBA were bound on the electrode surface through the formation of boronate ester bonds, then inducing the assembly of AgNPs. However, once the tyrosine residues were phosphorylated by Src with adenosine triphosphate (ATP) as the co-substrate, the phosphorylated peptides could not transform into o-diphenol moieties. As a result, the networks of AgNPs were not anchored onto the electrode surface. Hydrogen peroxide (H_2O_2) transform boronate group (either boronic acid or boronate ester) into its corresponding phenol form, losing the ability to interact with 1,2- or 1,3-diols. *p*-Benzenediboronic acid (BDBA) could induce the aggregation of citrate-capped Ag NPs through the cross-linking reaction between citrate and boronic acid of BDBA. Thus, Liu's group also designed a H_2O_2 electrochemical sensor based on the above mentioned mechanism [56]. Cucurbit[8]urils (CB[8]) with relative bigger cavity can combine with metal NPs and induce NPs aggregation, even after embedding more than one guest at a time [22, 62]. Song et. al utilized methylviologen/CB[8] complex to enhance the electrochemical signal through layer-by-layer assembly of AgNPs for sensitive detection of caspase-3 [63]. Caspase-3 could cleavage the substrate and exposure a free phenylalanine at the end of the peptide, further binding CB[8] specifically through host-guest reaction. The electrochemical signal of the AgNPs-CB[8]-AgNPs formed on the electrode surface could be further enhanced by methylviologen embedding in CB[8]. Hu et al. reported a sensitive assay for the detection of biothiols based biothiol-induced aggregation of AgNPs [64].

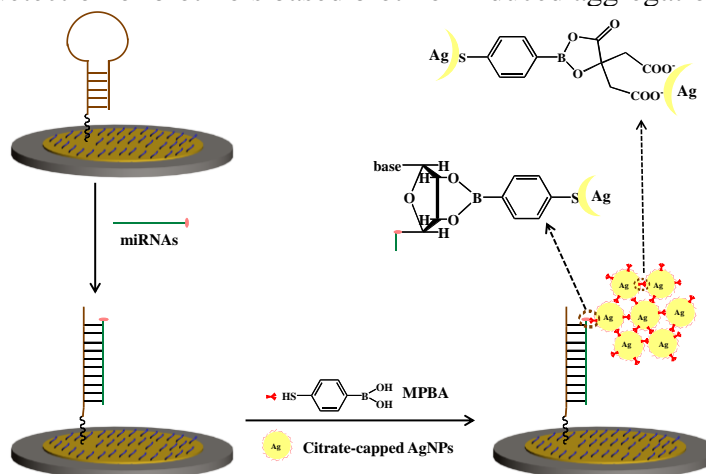


Figure 6. Schematic representation of the electrochemical strategy for miRNAs detection based on MPBA-induced in situ formation of AgNPs aggregates as labels. Reprinted with permission from [58].

2.4 AgNPs-based nanocomposites

To further improve the sensitivity of biosensors, various nanomaterials or polymeric microbeads have been exploited by means of externally (on their surface) or internally loading abundant AgNPs. Numerous Ag NPs are captured by the formed sandwich-like complex and then the

signal is further amplified by a subsequent Ag NP-promoted deposition of silver ions, resulting in a significantly amplified electrochemical-stripping signal of Ag NPs. Gao et al. prepared AgNPs-loaded multiwall carbon-nanotubes (MWNTs) (Ag-MWNTs) by electroless-plating as probes to sensitively detect DNA hybridization [65]. Ag-MCNTs then were modified with thiol group-functionalized ssDNA and hybridized with target ssDNA immobilized on the gold electrode surface. The direct electrochemical measurement of silver oxidation signal with potential interval from -100 to +300 mV was firstly used to monitor the DNA hybridization. Single-walled carbon nanotubes (SWCNTs) were utilized to carry AgNPs as an electrochemical label and AgNPs-SWCNTs nanohybrids could discriminate ssDNA and dsDNA, because the nitrogenous bases exposed outside of ssDNA had a stronger affinity toward SWCNTs than that embedded inside of dsDNA [66].

Graphene oxide (GO), as a derivate of graphene, have attracted increasing attention in recent years as a novel class of 2D carbon-based nanomaterials. Due to its large interfacial surface and high loading efficiency, GO have been widely used as nanocarrier to anchor different labels, such as enzymes and electroactive molecules [67]. Bai et al. in situ deposited Ag NPs on the surface of GO to produce GO-AgNPs nanocomposites and applied it as an electroactive tag to develop immunoassay for clenbuterol determination [68]. Jiang et al. prepared GO-AgNPs nanocomposites through self-assembly and further used it to detect *Escherichia coli* (*E. coli*) through a sandwich-type immunoassay [69]. Avian influenza virus H7 (AIV H7) can also be quantified by using GO-AgNPs-Chitosan nanocomposites as trace labels with a sandwich-type immunoassay format [70]. Carboxylated carbon nanocubes (CNCs) was used as a substrate for in situ growth of AgNPs to produce AgNPs-CNCs as a tracing tags and was labelled with anti-5-methylcytosine antibody for sensitive detection of DNA methylation and methyltransferase activity [71].

Graphene-like 2D molybdenum disulfide (MoS_2) nanosheets also has gained extensive attention because of its large surface area and comparatively high electron mobility. Wang et al. synthesized molybdenum disulfide (MoS_2) wrapped Fe_3O_4 NPs ($\text{MoS}_2@ \text{Fe}_3\text{O}_4$), assembled it with pre-synthesized AgNPs ($\text{Ag}/\text{MoS}_2@ \text{Fe}_3\text{O}_4$) and labelled it with Ab_2 [72]. After the typical immunoassay in the 96-well microplate, the unbound $\text{Ab}_2\text{-Ag}/\text{MoS}_2@ \text{Fe}_3\text{O}_4$ was collected and detected with the magnetic glassy carbon electrode (MGCE) by DPV. Due to easy and simple synthesis and high specific surface area, polydopamine nanospheres (PDANSs) have been utilized to load other molecules and materials, including DNA, AuNPs and Fe_3O_4 NPs [73-75]. Zhang et al. synthesized PDANSs by the one-step self-polymerization, in situ deposited AgNPs on PDANSs, labelled it with SA and employed the as-synthesized AgNPs/PDANSs nanocomposite as electrochemical labels for the ultrasensitive OTA aptasensor.

2.4 Nanomaterial-promoted reduction of silver ions

In recent years, electrochemical assays, based on silver deposition to further increase loading of electrochemically detectable metallic silver, has attracted considerable attention in signal amplification, because of high sensitivity, simplicity and easy implementation in biomedical application. This is very often completed on the basis of a seed-mediated nucleation/growth

mechanism by employing Ag or Au seeds to mediate the deposition of more Ag. This strategy has been valuable in the design of ultrasensitive biosensors by many groups.

The use of AuNPs as promoters for silver ions reduction has been popular in developing electrochemical and optical sensors for a large number of targets to improve the sensitivity of assays [76]. For example, Mirkin and co-workers have developed a colorimetric detection scheme for DNA [77]. In 2001, Wang et al. reported a novel method for detecting DNA hybridization based on the precipitation of silver on gold nanoparticle tags and a subsequent electrochemical stripping detection of the dissolved silver (Figure 7A) [3]. Next, Chu et al. applied this silver-enhanced AuNPs electrochemical stripping detection strategy to construct an electrochemical metalloimmunoassay [78]. However, the electrochemical methods based on silver enhancement always need an acid dissolution step to produce a solution containing a large amount of silver ions. Since Ting et al. explored the solid-state Ag/AgCl process to develop an electrochemical immunosensor in 2009, the utilization of this silver-enhanced AuNPs electrochemical stripping detection strategy has a new life [24, 79-81]. In this work, when Ab₂-labelled AgNPs was captured during the sandwich immunoassay, AgNPs-prommoted reduction of silver ions was triggered by the captured AgNPs with a silver developer solution containing AgNO₃, ascorbic acid (AA) and Tween 80. The electrode was then placed into 1 M KCl solution for cyclic voltammetric measurements. The solid-state Ag/AgCl voltammetry showed a more intensive peak current than the Ag stripping voltammetry in 1M KNO₃ solution. Next, Lai et al. design an electrochemical stripping method for multiplexed detection of CEA and AFP by using Ab₂-modified AuNPs as catalysts and nuclei to induce the silver deposition [82]. Gao et al. combined circular strand-displacement polymerization (CSRDP) with silver enhancement for sub-femtomolar electrochemical detection of DNA [83]. Wang et al. porposed amplified terminal protection assay of small molecule/protein interactions [84]. As a model of biotin/SA interaction, SA could protect biotin-modified ssDNA against hydrolysis by Exo I. Thus, the negatively charged ssDNA could electrostatically abosorb positively charged AuNPs, and AuNP-catalyzed silver enhancement and the solid-state Ag/AgCl process was conducted. However, in these assays, the chemically-reduced silver deposition could not discriminate the target molecules and the sensor surfaces, resulting in the nonspecific deposition of silver on the whole electrode surface and irreproducibility. To solve this problem, Zhu et al. synthesized the bioconjugate of hydrazine-AuNP-aptamer (Hyd-AuNP-Apt) as a nanoprobe to electrochemical diagnosis of breast cancer [85]. As shown in Figure 7B, after the formation of a sandwich-type structure, the depositon of silver ions on the bioconjugate was directly initiated by Hyd-AuNP-Apt without the addition of reductants. The deposited silver could be analyzed using square wave stripping voltammetry (SWSV) to quantify concentrations of HER2 or HER2-overexpressing cells.

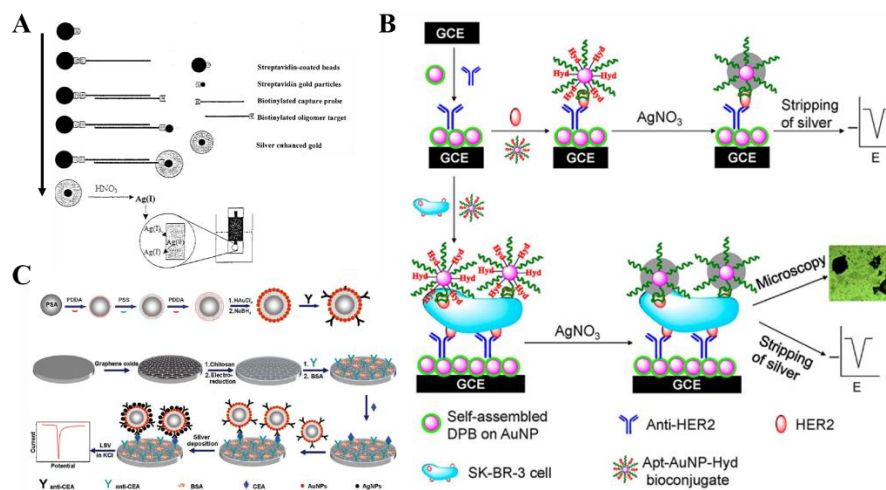


Figure 7. (A) Schematic representation of traditional silver-enhanced colloidal gold electrochemical stripping detection of DNA hybridization. Reprinted with permission from [3]. Copyright 2001 American Chemical Society. (B) Schematic representation of the immunosensor for detection of HER2 protein and HER2-overexpressing SK-BR-3 breast cancer cells. Reprinted with permission from [85]. Copyright 2013 American Chemical Society. (C) Schematic representation of the preparation of tracing tag and labeled Ab_2 , and immunosensor fabrication and sandwich-type immunoassay procedure. Reprinted with permission from [86]. Copyright 2012 American Chemical Society.

Moreover, like the strategy presented in Section 2.3, other nanomaterials could be utilized as substrates to carry NPs. The formed hybrids could improve the stability of NPs during the modification procedure and improve the sensitivity of assays because of the high content of Ag NPs on every one tracing tag. Lai et al. develop immunoassay for multiplexed detection of tumor markers by *in situ* deposition of AgNPs on carboxylated CNTs [87]. The proposed assay showed a LOD down to sub-picomogram per milliliter level. Lin et al. designed a triple signal amplification strategy for ultrasensitive electrochemical immunosensing of carcinoembryonic antigen (CEA) [86]. As shown in Figure 7C, the electrochemically-reduced GO was modified on the electrode surface to accelerate electron transfer. AuNPs on the surface of poly(styrene-co-acrylic acid) microbead were used to label Ab_2 and induce silver deposition for ASV analysis. The proposed method had a linear range of 0.5 pg mL^{-1} to 0.5 ng mL^{-1} and a LOD down to 0.12 pg mL^{-1} . Moreover, mesoporous carbon foam [88], carbon nanohorn [89], polypyrrole microspheres [90], Fe_3O_4 NPs [91] and C_{60} -modified polyamidoamine dendrimers [92] were used to carry AuNPs as a novel signal tags to induce silver enhancement for the fabrication of electrochemical immunosensors.

Recently, carbon materials, such as GO and carbon nanotubes (CNTs), have been reported to facilitate and catalyze the silver deposition. Wan et al. demonstrated that GO could catalyze the reduction of $\text{Ag}(\text{I})$ into Ag metal by hydroquinone (HQ), and applied GO-mediated Ag enhancement to detect bacteria (Figure 8) [93]. In this work, after sulfate-reducing bacteria (SRBs) were captured, the anti-SRB Ab-functionalized GO conjugates as biocatalytic probes were added to label SRBs. Upon the addition of silver ions and HQ, Ag was well deposited onto the surface of GO, which could be detected by potentiometric stripping analysis to quantify the concentration of SRB. The targeted bacteria was

detected at 1.8×10^2 to 1.8×10^8 cfu mL⁻¹ concentration range. GO can absorb ssDNA through the π - π interaction and the binding affinity is stronger than that of dsDNA. Tang et al. constructed a label free electrochemical sensor for Pb²⁺ based on GO-mediated deposition of AgNPs [94]. In the presence of Pb²⁺, the aptamer in dsDNA on the electrode surface transformed into a stable G-quadruplex structure and the left ssDNA capture probe could recruit GO. Then, AgNPs was catalytically deposited on the surface of GO. Based on similar strategy, DNA from cauliflower mosaic virus 35S was detected over a wide range from 10 fM to 10 nM with a LOD of 7.6 fM [95]. Meanwhile, GO can absorb peptides by interaction with benzene ring moiety of aromatic amino acids of peptides. Thus, Meng et al. fabricated a peptide cleavage-based electrochemical biosensor based on GO-promoted AgNPs deposition [95]. Once PSA was added, the peptide modified on the electrode was specifically cleaved and liberated GO, then resulting in the inhibition of AgNPs *in situ* deposition and the decrease of the electrochemical stripping signal.

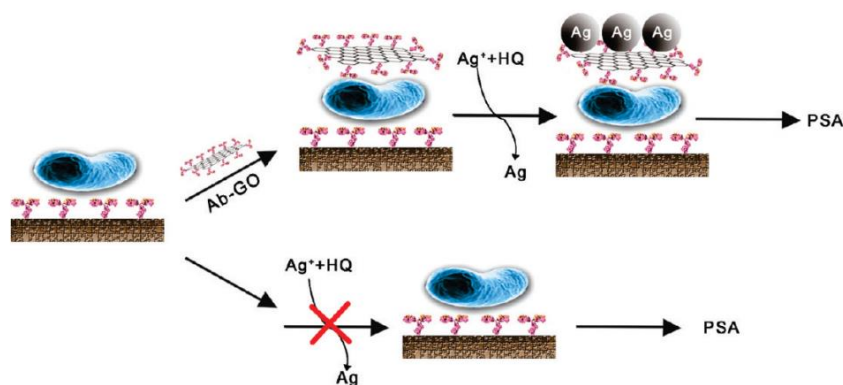


Figure 8. Schematic representation of this new detection method for sulphate-reducing bacteria (SRB) based on the GO sheet-amplified immunoassay combined with the silver enhancement. Reprinted with permission from [93]. Copyright 2011 American Chemical Society.

2.6 DNA-based biometallization

Biomineralization, which refers to the biologically-controlled formation of mineral deposits, can serve as a powerful strategy to synthesize metal NPs. DNA is rich of phosphate groups, amino groups and heterocyclic nitrogen atom, which offers multiple binding sites for positively charged silver ions, following reduced to form metallic cluster. Thus, DNA has been used as a controllable and adaptable biomineralization template. DNA-templated growth of AgNPs has led to several optical and electrochemical methods [4, 96].

Wu et al. combined DNA-templated deposition of AgNPs as electroactive labels with ExoIII-assisted background current suppression to sensitively monitor telomerase activity detection in circulating tumor cells [97]. In the presence of telomerase and dNTPs mixture, the the telomerase primer oligonucleotides (TS) was elongated and the negative charge of the electrode surface increased, resulting in higher degree of DNA metallization and more AgNPs formed on the surface. Thus, the magnitude of the peak currents depended on the extended degree of TS by telomerase, thus could be used for telomerase activity sensing. However, in the absence of telomerase, after the

hybridization of TS primer and its complementary DNA, the TS primer would have a blunt 3'-terminus, which initiated the ExoIII-assisted the complementary DNA recycling and resulting in complete removing of unextended primer. Thus, a striking high-signal-to-noise ratio was achieved. The constructed biosensor exhibited comparable sensitivity with the conventional telomeric repeat amplification protocol (TRAP). Qian et al. reported a label-free and enzyme-free electrochemical aptasensor based on DNA in situ silver metallization, and the ingenious combination of target catalyzed hairpin assembly and HCR [98]. Recently, Sueba-Ngam et al. designed an electroanalytical aptasensor for precise determination of ochratoxin A (OTA) at trace levels [99]. In this study (Figure 9), the OTA aptamer was modified on the electrode to capture OTA and further produce silver metallization as a signal enhancer. Exonuclease I was utilized to digest unbound OTA aptamer, and reduced nonspecific background metallization and enhanced analytical sensitivity. The developed electrochemical aptasensor had a linear range between 0.001 and 100 ng mL⁻¹ and an LOD of 0.7 pg mL⁻¹. Sueba-Ngam et al. confirmed that ssDNA could mediate the growth of AgNPs on the surface of SWCNTs and realized T2DM-related SNP assay coupled with RNase HII enzyme assisted amplification [100].

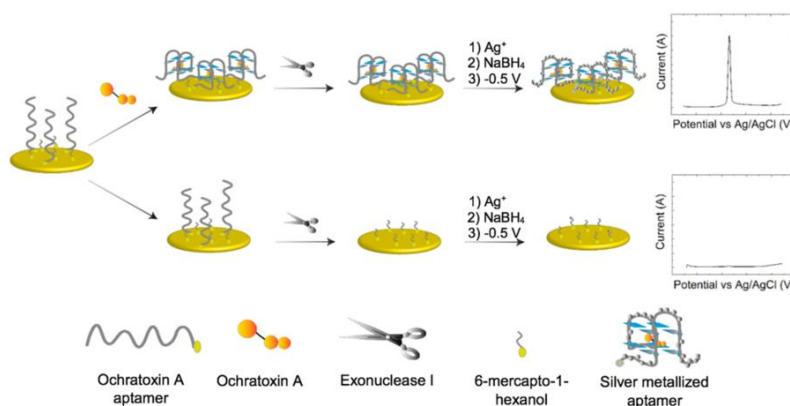


Figure 9. Schematic illustration of the silver metallization assay for OTA detection using enzyme-assisted background current suppression. Reprinted with permission from [99]. Copyright 2019 American Chemical Society.

The non-specific adsorption of positively charged silver ions onto the negatively charged phosphodiester backbone of ssDNA and dsDNA causes high background signal and low signal-to-noise ratio. As a DNA analog, peptide nucleic acid (PNA) with a neutral backbone has been utilized by researchers to achieve the comparatively reduced background signal, because only PNA/DNA heteroduplexes could electrostatically absorb metal ions for metallization. For example, Li et al. reported an electroanalytical strategy for microRNAs by using PNAs as capture probes [101]. Moreover, the silver deposition was induced by the synergic photocatalysis of TiO₂ and the photoreduction of guanine bases on the target miRNAs, avoiding of use of additional reductants. Hu et al. designed a PNA-based DNA assay based on PNA and polygalacturonic acid (PGUA) mediated in-situ deposition of AgNPs [102]. After the hybridization of PNA and target DNA, PGUA was bound by using zirconium ions as bridge via phosphate-zirconiumcarboxylate coordination interaction. Then, the vicinal hydroxy groups of PGUA were cleaved and oxidized into aldehyde groups by NaIO₄, which in

turn reduce Ag ions into AgNPs. Thus, the amount of target ssDNA was proportionally correlated with the deposited AgNPs, and could be analyzed by DPV in a solution of KCl. More recently, they combined DNA-templated deposition of AgNPs with electrochemically mediated polymerization signal amplification to design ultrasensitive biosensors for DNA detection (Figure 10A) [103]. For instance, after the chain transfer agent, 4-cyano-4-(phenylcarbonothioylthio)pentanoic acid (CPAD), was linked to the heteroduplex of PNA/DNA by the coordination bonding of Zr^{4+} , electrochemically mediated reversible addition–fragmentation chain transfer (eRAFT) was initiated on the surface of the electrode [104]. The principle of eRAFT is shown in Figure 10B. Then, glycosyloxyethyl methacrylates (GEMA) were transformed into a polymer-containing sugar glucose. Following the oxidation by $NaIO_4$ and the silver mirror reaction, AgNPs were deposited on the electrode surface and quantified by DPV. Under the optimal conditions, the sensor showed a good linear relationship in the range of 10 aM to 10 pM and the LOD as low as 4.725 aM.

Based on DNA-metallization, specifically designed DNA sequence as template can be used *in situ* synthesize fluorescent silver nanoclusters (AgNCs) instead of larger size AgNPs, which have been utilized as effective electrochemical probes [105–107]. By loading C-rich ssDNA on AuNPs, after a sandwich-type structure formed, AgNCs were synthesized by using ssDNA as template and produced the direct voltametric signal for the detection of target DNA [108]. Peng and co-workers reported label-free electrochemical sensing of methyltransferase activity by the HCR amplification strategy and *in situ* growth of DNA-templated AgNCs [109].

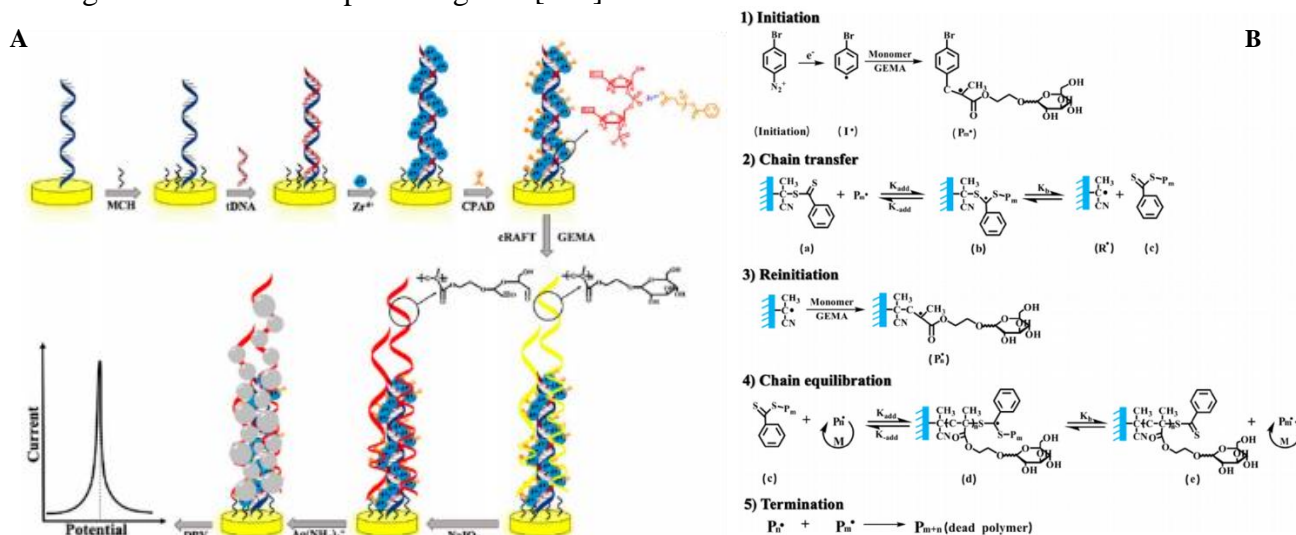


Figure 10. Schematic illustration of (A) the electrochemical detection of DNA based eRAFT and *in situ* metallization dual-signal amplification and (B) the eRAFT-polymerization-based amplification strategy. Reprinted with permission from [103] and [104]. Copyright 2019 American Chemical Society.

2.6 ALP-catalyzed silver deposition

In the conventional metal enhancement process, sometimes, Ag deposition can occur slowly, even in the absence of the nanoparticle catalyst, which significantly increases background levels and

decreases the reproducibility of electrochemical signal levels. Aiming to solve this problem, enzyme-catalyzed silver deposition, which is highly specific silver deposition at the presence of enzyme and corresponding substrates, has been innovatively used for signal amplification of detectable optical and electrochemical signal. This method has a significant increase in sensitivity and without the background.

As one of the most used enzymes, ALP can hydrolyze nonelectroactive substrates such as *p*-aminophenyl phosphate (*p*-APP), 3-indoxyl phosphate (3-IP), and ascorbic acid 2-phosphate (2-PAA) into reducing agents which can reduce silver ions to produce electroactive Ag deposition [110-112]. For example, Hwang et al. reported a electrochemical system for DNA detection based on stripping voltammetry of enzymatically deposited silver [113]. After the target DNA hybridized with biotinylated detection DNA probe and capture DNA probe on the electrode surface, neutravidin-conjugated alkaline phosphatase (Av-ALP) was captured and induced the Ag deposition in the presence of *p*-APP. Finally, the stripping current of the accumulated metal is measured using ASV. Similarly, an electrochemical amplification immunoassay based on ALP-labelled antibody and biocatalytic metal deposition was developed by Yu and co-workers [114]. For achieving a higher signal amplification, ALP-catalyzed hydrolysis can be further combined with the redox cycling of the enzyme product. For example, the chemical-chemical (CC) redox cycling of an enzyme product *p*-aminophenyl (AP) by reduced b-nicotinamide adenine dinucleotide (NADH) was employed to combine with ALP-catalyzed Ag deposition for the detection of creatine kinase-MB [115]. During the redox cycling, the enzyme product AP is oxidized into 4-quinone imine by silver ions and then regenerated by the added NADH. Compared with using only enzymatic Ag deposition, the method using redox cycling-amplified enzymatic Ag deposition showed a higher Ag-deposition rate. Another efficient strategy to improve the sensitivity is to combine ALP-catalyzed Ag deposition with various powerful DNA-amplification approaches, which have also been introduced in above section [116-118].

However, silver deposition on the electrode may inhibit the activity of the enzyme and block the continual deposition of Ag [119]. Meanwhile, the prepared labels can greatly amplify the transduction signal of a recognition event in bioassays by loading ALP on NPs. For example, silica nanoparticles were used to carry ALP and antibody for the detection of PSA in human serum [120]. Among kinds of carriers, AuNPs have been often utilized, acting as both deposition sites and catalysts for the reduction of Ag⁺ to metallic Ag [121]. Lai et al. proposed a novel multiplexed immunoassay method by the intergration of ALP-labeled Ab-modified AuNPs (ALP-Ab/Au NPs) and enzyme-AuNP catalyzed Ag deposition (Figure 11A) [122]. After sandwich-type immunoreactions, the ALP-Ab/Au NPs were captured on an immunosensor surface to catalyze the hydrolysis of 3-IP into an indoxyl intermediate to reduce Ag cations. The high content enzyme in a single recognition event and AuNP-accelerated enzyme-catalyzed Ag deposition provided high sensitivity with signal amplification. Moreover, the hydrolysis product of ALP substrate could be quickly oxidized by sufficient silver cation surrounding the working electrode, which excluded completely the cross talk between adjacent immunosensors. This multiplexed immunoassay showed wide linear ranges over 4 orders of magnitude with the LODs down to 4.8 and 6.1 pg/mL for human and mouse IgG, respectively. Si et al. demonstrated that ALP-templated gold nanoclusters (ALP-AuNCs) possessed dramatically enhanced catalysis activity than native ALP (Figure 11B) [123]. When applied into the enzyme-catalyzed Ag deposition, the ALP-

AuNC labels could act as the bicatalysts toward substrate dephosphorylation reaction and the accelerator in Ag deposition reaction. The developed ALP-AuNCs-based electrochemical method exhibited a linear detection range from 0.014 to 20.0 fM with the LOD as low as 4.61 aM.

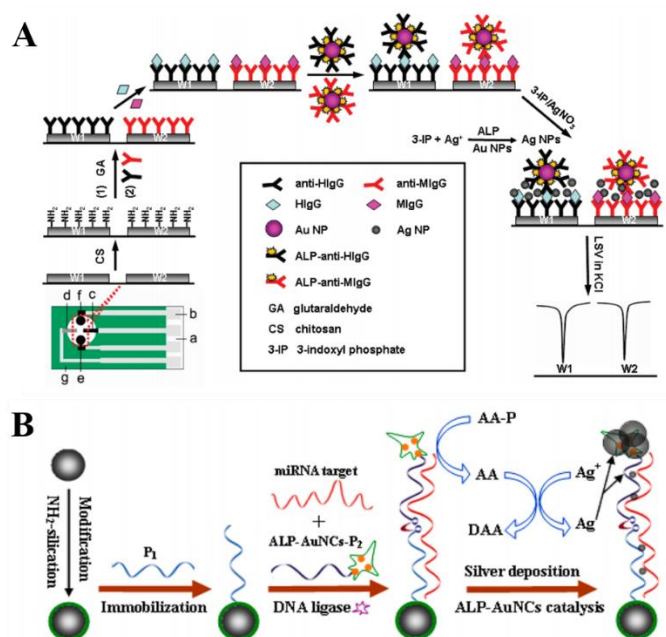


Figure 11. (A) Schematic representation of preparation of immunosensor array and detection strategy by sandwich-type immunoassay and linear sweep voltammetric stripping analysis of enzymatically deposited Ag NPs. Reprinted with permission from [122]. Copyright 2011 American Chemical Society. (B) Schematic illustration of the principle for the sandwich-type electroanalysis of miRNAs based on the ALP-AuNCs-catalyzed silver deposition. Reprinted with permission from [123]. Copyright 2014 American Chemical Society.

3. CONCLUSION

This review demonstrated the applications of AgNPs for signal amplification transduction of biorecognition events. By combining the excellent properties of AgNPs with various new DNA-based amplification technologies, ultrasensitive detection of disease markers, drugs, cells and enzymes was achieved. However, it should be pointed out that there still exist some challenges to overcome in biosensing applications. For example, the stability and reproducibility greatly limit the practical applications of AgNPs-based electrochemical biosensors.

ACKNOWLEDGMENTS

Partial support of this work by the National Natural Science Foundation of China (21401006, U1304210) and the Program for Science and Technology Innovation Talents at the University of Henan Province (16HASTIT006).

References

1. N. Xia, D. Deng, X. Mu, A. Liu, J. Xie, D. Zhou, P. Yang, Y. Xing and L. Liu, *Sens. Actuat. B: Chem.*, 306 (2020) 127571.
2. L. Authier, C. Grossiord and P. Brossier, *Anal. Chem.*, 73 (2001) 4450.
3. J. Wang, R. Polsky and D. Xu, *Langmuir*, 17 (2001) 5739.
4. J. Wang, O. Rincon, R. Polsky and E. Dominguez, *Electrochem. Commun.*, 5 (2003) 83.
5. L. N. Feng, J. Peng, Y. D. Zhu, L. P. Jiang and J. J. Zhu, *Chem. Commun.*, 48 (2012) 4474.
6. L. N. Feng, Z. P. Bian, J. Peng, F. Jiang, G. H. Yang, Y. D. Zhu, D. Yang, L. P. Jiang and J. J. Zhu, *Anal. Chem.*, 84 (2012) 7810.
7. F. F. Cheng, T. T. He, H. T. Miao, J. J. Shi, L. P. Jiang and J. J. Zhu, *ACS Appl. Mater. Interfaces*, 7 (2015) 2979.
8. P. Sun, W. W. Xiong, D. Zhu, Z. Dong, X. Jin, B. Liu, Y. Zhang, B. Bao, W. Yao, L. Zhang and F. F. Cheng, *Analyst*, 143 (2018) 5170.
9. T. Z. Liu, R. Hu, X. Zhang, K. L. Zhang, Y. Liu, X. B. Zhang, R. Y. Bai, D. Li and Y. H. Yang, *Anal. Chem.*, 88 (2016) 12516.
10. M. Chen, N. Gan, Y. Zhou, T. Li, Q. Xu, Y. Cao and Y. Chen, *Sens. Actuat. B: Chem.*, 242 (2017) 1201.
11. P. Zhang, H. Huang, N. Wang, H. Li, D. Shen and H. Ma, *Microchim. Acta*, 184 (2017) 4037.
12. Y. Yang, J. Cheng, B. Wang, Y. Guo, X. Dong and J. Zhao, *Microchim. Acta*, 186 (2019) 101.
13. G. Yuan, C. Yu, C. Xia, L. Gao, W. Xu, W. Li and J. He, *Biosens. Bioelectron.*, 72 (2015) 237.
14. H. Gao, X. Jiang, Y. J. Dong, W. X. Tang, C. Hou and N. N. Zhu, *Biosens. Bioelectron.*, 48 (2013) 210.
15. Z. Wang, N. Liu, F. Feng and Z. Ma, *Biosens. Bioelectron.*, 70 (2015) 98.
16. J. Wang, D. Xu, A. N. Kawde and R. Polsky, *Anal. Chem.*, 73 (2001) 5576.
17. M. Dequaire, C. Degrand and B. Limoges, *Anal. Chem.*, 72 (2000) 5521.
18. J. A. Ho, H. C. Chang, N. Y. Shih, L. C. Wu, Y. F. Chang, C. C. Chen and C. Chou, *Anal. Chem.*, 82 (2010) 5944.
19. O. S. Ivanova and F. P. Zamborini, *J. Am. Chem. Soc.*, 132 (2010) 70.
20. H. Cai, Y. Xu, N. Zhu, P. He and Y. Fang, *Analyst*, 127 (2002) 803.
21. J. Wang, D. Xu and R. Polsky, *J. Am. Chem. Soc.*, 124 (2002) 4208.
22. S. Mahajan, T. C. Lee, F. Biedermann, J. T. Hugall, J. J. Baumberg and O. A. Scherman, *Phys. Chem. Chem. Phys.* 12 (2010) 10429.
23. J. Zhang, B. P. Ting, N. R. Jana, Z. Gao and J. Y. Ying, *Small*, 5 (2009) 1414.
24. B. P. Ting, J. Zhang, M. Khan, Y. Y. Yang and J. Y. Ying, *Chem. Commun.* (2009) 6231.
25. P. Singh, K. L. Parent and D. A. Buttry, *J. Am. Chem. Soc.*, 134 (2012) 5610.
26. B. P. Ting, J. Zhang, Z. Gao and J. Y. Ying, *Biosens. Bioelectron.*, 25 (2009) 282.
27. J. Zhuang, L. Fu, M. Xu, H. Yang, G. Chen and D. Tang, *Anal. Chim. Acta*, 783 (2013) 17.
28. F. Gao, Y. Du, J. Yao, Y. Zhang and J. Gao, *RSC Adv.*, 5 (2015) 9123.
29. P. Miao, Y. Tang, Q. Zhang, B. Bo and J. Wang, *ChemPlusChem*, 80 (2015) 1712.
30. P. Miao, F. Meng, B. Wang, X. Zhu and Y. Tang, *Electrochem. Commun.*, 51 (2015) 89.
31. Y. Wen, H. Pei, Y. Wan, Y. Su, Q. Huang, S. Song and C. Fan, *Anal. Chem.*, 83 (2011) 7418.
32. H. Pei, N. Lu, Y. Wen, S. Song, Y. Liu, H. Yan and C. Fan, *Adv. Mater.*, 22 (2010) 4754.
33. P. Miao, B. Wang, F. Meng, J. Yin and Y. Tang, *Bioconjug. Chem.*, 26 (2015) 602.
34. P. Miao, Y. Jiang, Y. Wang, J. Yin and Y. Tang, *Sens. Actuat. B: Chem.*, 257 (2018) 1021.
35. P. Miao, B. Wang, X. Chen, X. Li and Y. Tang, *ACS Appl. Mater. Interfaces*, 7 (2015) 6238.
36. J. Wang, J. Yu, X. Zhou and P. Miao, *ChemElectroChem*, 4 (2017) 1828.
37. H. Chai and P. Miao, *Anal. Chem.* 91 (2019) 4953.
38. L. Ma, D. Ning, H. Zhang and J. Zheng, *Biosens. Bioelectron.*, 68 (2015) 175.

39. N. Hao, H. Li, Y. Long, L. Zhang, X. Zhao, D. Xu and H.-Y. Chen, *J. Electroanal. Chem.*, 656 (2011) 50.
40. C. Yin, G. Lai, L. Fu, H. Zhang and A. Yu, *Electroanalysis*, 26 (2014) 409.
41. S. Yazdanparast, A. Benvidi, M. Banaei, H. Nikukar, M. D. Tezerjani and M. Azimzadeh, *Microchim. Acta*, 185 (2018) 405.
42. F. Meng, K. Han, B. Wang, T. Liu, G. Liu, Y. Li and P. Miao *ChemistrySelect*, 1 (2016) 1515.
43. J. Zhang, H. Chen, Y. Cao, C. Feng, X. Zhu and G. Li, *Anal. Chem.*, 91 (2019) 1005.
44. Y. Tang, Y. Dai, X. Huang, L. Li, B. Han, Y. Cao and J. Zhao, *Anal. Chem.*, 91 (2019) 7531.
45. P. Miao, K. Han, H. Sun, J. Yin, J. Zhao, B. Wang and Y. Tang, *ACS Appl. Mater. Interfaces*, 6 (2014) 8667.
46. L. Cui, J. Wu, J. Li, Y. Ge and H. Ju, *Biosens. Bioelectron.*, 55 (2014) 272.
47. T. Wei, T. Dong, Z. Wang, J. Bao, W. Tu and Z. Dai, *J. Am. Chem. Soc.*, 137 (2015) 8880.
48. H. Li, Z. Sun, W. Zhong, N. Hao, D. Xu and H. Y. Chen, *Anal. Chem.*, 82 (2010) 5477.
49. W. Song, H. Li, H. Liang, W. Qiang and D. Xu, *Anal. Chem.*, 86 (2014) 2775.
50. X. Jiang, K. Chen and H. Han, *Biosens. Bioelectron.*, 28 (2011) 464.
51. M. Zhou, L. Han, D. Deng, Z. Zhang, H. He, L. Zhang and L. Luo, *Sens. Actuat. B: Chem.*, 291 (2019) 164.
52. S.-H. Wen, R.-P. Liang, L. Zhang and J.-D. Qiu, *ACS Sustain. Chem. Eng.*, 6 (2018) 6223.
53. Y. Zhao, L. Cui, W. Ke, F. Zheng and X. Li, *ACS Sustain. Chem. Eng.*, 7 (2019) 5157.
54. X. Wu, Z. Li, X. X. Chen, J. S. Fossey, T. D. James and Y. B. Jiang, *Chem. Soc. Rev.*, 42 (2013) 8032.
55. M. Li, W. Zhu, F. Marken and T. D. James, *Chem. Commun.*, 51 (2015) 14562.
56. L. Liu, T. Sun and H. Ren, *Materials*, 10 (2017)
57. N. Xia, X. Wang, B. Zhou, Y. Wu, W. Mao and L. Liu, *ACS Appl. Mater. Interfaces*, 8 (2016) 19303.
58. N. Xia, C. Cheng, L. Liu, P. Peng, C. Liu and J. Chen, *Microchim. Acta*, 184 (2017) 4393.
59. L. Liu, Y. Chang, N. Xia, P. Peng, L. Zhang, M. Jiang, J. Zhang and L. Liu, *Biosens. Bioelectron.*, 94 (2017) 235.
60. N. Xia, L. Liu, Y. Chang, Y. Hao and X. Wang, *Electrochem. Commun.*, 74 (2017) 28.
61. L. Liu, C. Cheng, Y. Chang, H. Ma and Y. Hao, *Sens. Actuat. B: Chem.*, 248 (2017) 178.
62. S. Kasera, F. Biedermann, J. J. Baumberg, O. A. Scherman and S. Mahajan, *Nano Lett.*, 12 (2012) 5924.
63. S. Song, X. Hu, H. Li, J. Zhao, K. Koh and H. Chen, *Sens. Actuat. B: Chem.*, 274 (2018) 54.
64. L. Hu, S. Hu, L. Guo, T. Tang and M. Yang, *Anal. Methods*, 8 (2016) 4903.
65. M. Gao, H. Qi, Q. Gao and C. Zhang, *Electroanalysis*, 20 (2008) 123.
66. A. Asadzadeh-Firouzabadi and H. R. Zare, *Sens. Actuat. B: Chem.*, 260 (2018) 824.
67. N. Xia, D. Deng, S. Yang, Y. Hao, L. Wang, Y. Liu, C. An, Q. Han and L. Liu, *Sens. Actuat. B: Chem.*, 291 (2019) 113.
68. J. Bai, Y. Lai, D. Jiang, Y. Zeng, Y. Xian, F. Xiao, N. Zhang, J. Hou and L. Jin, *Analyst*, 137 (2012) 4349.
69. X. Jiang, K. Chen, J. Wang, K. Shao, T. Fu, F. Shao, D. Lu, J. Liang, M. F. Foda and H. Han, *Analyst*, 138 (2013) 3388.
70. J. Huang, Z. Xie, Z. Xie, S. Luo, L. Xie, L. Huang, Q. Fan, Y. Zhang, S. Wang and T. Zeng, *Anal. Chim. Acta*, 913 (2016) 121.
71. F. Gao, T. Fan, S. Ou, J. Wu, X. Zhang, J. Luo, N. Li, Y. Yao, Y. Mou, X. Liao and D. Geng, *Biosens. Bioelectron.*, 99 (2018) 201.
72. Y. Wang, G. Zhao, Y. Zhang, X. Pang, W. Cao, B. Du and Q. Wei, *Sens. Actuat. B: Chem.*, 266 (2018) 561.
73. L. Liu, Y. Chang, J. Yu, M. Jiang and N. Xia, *Sens. Actuat. B: Chem.*, 251 (2017) 359.
74. Y. X. Dong, J. T. Cao, Y. M. Liu and S. H. Ma, *Biosens. Bioelectron.*, 91 (2017) 246.

75. J. Yan, L. Yang, M. F. Lin, J. Ma, X. Lu and P. S. Lee, *Small*, 9 (2013) 596.
76. S. J. Park, T. A. Taton and C. A. Mirkin, *Science*, 295 (2002) 1503.
77. T. A. Taton, C. A. Mirkin and R. L. Letsinger, *Science*, 289 (2000) 1757.
78. X. Chu, X. Fu, K. Chen, G. L. Shen and R. Q. Yu, *Biosens. Bioelectron.*, 20 (2005) 1805.
79. J. Li, J. Wu, L. Cui, M. Liu, F. Yan and H. Ju, *Analyst*, 141 (2016) 131.
80. J. Tang, Y. Huang, C. Zhang, H. Liu and D. Tang, *Microchim. Acta*, 183 (2016) 1805.
81. P. Duangkaew, T. Wutikhun and R. Laocharoensuk, *Sens. Actuat. B: Chem.*, 239 (2017) 430.
82. G. Lai, L. Wang, J. Wu, H. Ju and F. Yan, *Anal. Chim. Acta*, 721 (2012) 1.
83. F. Gao, Z. Zhu, J. Lei, Y. Geng and H. Ju, *Biosens. Bioelectron.*, 39 (2013) 199.
84. Q. Wang, B. Jiang, J. Xu, J. Xie, Y. Xiang, R. Yuan and Y. Chai, *Biosens. Bioelectron.*, 43 (2013) 19.
85. Y. Zhu, P. Chandra and Y. B. Shim, *Anal. Chem.*, 85 (2013) 1058.
86. D. Lin, J. Wu, M. Wang, F. Yan and H. Ju, *Anal. Chem.*, 84 (2012) 3662.
87. G. Lai, J. Wu, H. Ju and F. Yan, *Adv. Funct. Mater.*, 21 (2011) 2938.
88. D. Lin, J. Wu, H. Ju and F. Yan, *Biosens. Bioelectron.*, 52 (2014) 153.
89. C. Zhao, J. Wu, H. Ju and F. Yan, *Anal. Chim. Acta*, 847 (2014) 37.
90. J. Zhang, Z. Xiong and Z. Chen, *Sens. Actuat. B: Chem.*, 246 (2017) 623.
91. M. Shamsipur, M. Emami, L. Farzin and R. Saber, *Biosens. Bioelectron.*, 103 (2018) 54.
92. P. Chen, T. Wang, X. Zheng, D. Tian, F. Xia and C. Zhou, *New J. Chem.*, 42 (2018) 4653.
93. Y. Wan, Y. Wang, J. Wu and D. Zhang, *Anal. Chem.*, 83 (2011) 648.
94. S. Tang, P. Tong, X. You, W. Lu, J. Chen, G. Li and L. Zhang, *Electrochim. Acta*, 187 (2016) 286.
95. N. Gao, F. Gao, S. He, Q. Zhu, J. Huang, H. Tanaka and Q. Wang, *Anal. Chim. Acta*, 951 (2017) 58.
96. Y. Lin, Y. Tao, F. Pu, J. Ren and X. Qu, *Adv. Funct. Mater.*, 21 (2011) 4565.
97. L. Wu, J. Wang, J. Ren and X. Qu, *Adv. Funct. Mater.*, 24 (2014) 2727.
98. Y. Qian, F. Gao, L. Du, Y. Zhang, D. Tang and D. Yang, *Biosens. Bioelectron.*, 74 (2015) 483.
99. A. Suea-Ngam, P. D. Howes, C. Stanley and A. J. deMello, *ACS Sens.* (2019)
100. J. Tao, P. Zhao, J. Zheng, C. Wu, M. Shi, J. Li, Y. Li and R. Yang, *Chem. Commun.*, 51 (2015) 15704.
101. R. Li, S. Li, M. Dong, L. Zhang, Y. Qiao, Y. Jiang, W. Qi and H. Wang, *Chem. Commun.*, 51 (2015) 16131.
102. Q. Hu, W. Hu, J. Kong and X. Zhang, *Microchim. Acta*, 182 (2014) 427.
103. H. Sun, J. Kong, Q. Wang, Q. Liu and X. Zhang, *ACS Appl. Mater. Interfaces*, 11 (2019) 27568.
104. H. Sun, W. Xu, B. Liu, Q. Liu, Q. Wang, L. Li, J. Kong and X. Zhang, *Anal. Chem.*, 91 (2019) 9198.
105. Z. Chen, C. Liu, F. Cao, J. Ren and X. Qu, *Chem. Soc. Rev.*, 47 (2018) 4017.
106. H. Dong, S. Jin, H. Ju, K. Hao, L. P. Xu, H. Lu and X. Zhang, *Anal. Chem.*, 84 (2012) 8670.
107. C. Guo, F. Su, Y. Song, B. Hu, M. Wang, L. He, D. Peng and Z. Zhang, *ACS Appl. Mater. Interfaces*, 9 (2017) 41188.
108. Y. Ye, Y. Liu, S. He, X. Xu, X. Cao, Y. Ye and H. Zheng, *Sens. Actuat. B: Chem.*, 272 (2018) 53.
109. X. Peng, J. Zhu, W. Wen, T. Bao, X. Zhang, H. He and S. Wang, *Biosens. Bioelectron.*, 118 (2018) 174.
110. K. Feng, J. Zhao, Z. S. Wu, J. Jiang, G. Shen and R. Yu, *Biosens. Bioelectron.*, 26 (2011) 3187.
111. J. Liu, X. Yuan, Q. Gao, H. Qi and C. Zhang, *Sens. Actuat. B-Chem.*, 162 (2012) 384.
112. R. C. B. Marques, E. Costa-Rama, S. Viswanathan, H. P. A. Nouws, A. Costa-García, C. Delerue-Matos and M. B. González-García, *Sens. Actuat. B: Chem.*, 255 (2018) 918.
113. S. Hwang, E. Kim and J. Kwak, *Anal. Chem.*, 77 (2005) 579.
114. Z.-P. Chen, Z.-F. Peng, J.-H. Jiang, X.-B. Zhang, G.-L. Shen and R.-Q. Yu, *Sens. Actuat. B: Chem.*, 129 (2008) 146.

115. A. M. Jiaul Haque, J. Kim, G. Dutta, S. Kim and H. Yang, *Chem. Commun.*, 51 (2015) 14493.
116. Y. Qian, C. Wang and F. Gao, *Biosens. Bioelectron.*, 63 (2015) 425.
117. L. Tong, J. Wu, J. Li, H. Ju and F. Yan, *Analyst*, 138 (2013) 4870.
118. W. Wang, T. Bao, X. Zeng, H. Xiong, W. Wen, X. Zhang and S. Wang, *Biosens. Bioelectron.*, 91 (2017) 183.
119. Z. P. Chen, J. H. Jiang, X. B. Zhang, G. L. Shen and R. Q. Yu, *Talanta*, 71 (2007) 2029.
120. N. Xia, D. Deng, X. Mu, A. Liu, J. Xie, D. Zhou, P. Yang, Y. Xing, L. Liu, *Sens. Actuat. B-Chem.*, 306 (2020) 127571.
121. W. Lai, D. Tang, X. Que, J. Zhuang, L. Fu and G. Chen, *Anal. Chim. Acta*, 755 (2012) 62.
122. G. Lai, F. Yan, J. Wu, C. Leng and H. Ju, *Anal. Chem.*, 83 (2011) 2726.
123. Y. Si, Z. Sun, N. Zhang, W. Qi, S. Li, L. Chen and H. Wang, *Anal. Chem.*, 86 (2014) 10406.

© 2020 The Authors. Published by ESG (www.electrochemsci.org). This article is an open access article distributed under the terms and conditions of the Creative Commons Attribution license (<http://creativecommons.org/licenses/by/4.0/>).